Supplementary Information (SI) for New Journal of Chemistry.
This journal is © The Royal Society of Chemistry and the Centre National de la Recherche Scientifique 2025

Re-engineering of FOX-7 Structure: Computational Assessment of Structural Modifications on Explosive Performance and Safety

Kalpana Sharma,[a] Rimpi Devi,[a] Vikas D. Ghule*[a] and Srinivas Dharavath[b]

[a]Department of Chemistry, National Institute of Technology Kurukshetra, Kurukshetra-136119, Haryana, India. E-mail: gvd@nitkkr.ac.in

[b]Energetic Materials Laboratory, Department of Chemistry, Indian Institute of Technology Kanpur, Kanpur-208016, Uttar Pradesh, India.

Computational details

Computations were carried out using the Gaussian 09 program suite[1]. The structure optimizations are performed with M06-2X/def2-TZVPP and characterized to be true local energy minima on the potential energy surface and no imaginary frequencies were found. Heat of formation (*HOF*) is a measure of energy content of an energetic material that can decompose, ignite and explode by heat or impact. It enters into the calculation of explosive and propellant properties such as detonation velocity, detonation pressure, heat of detonation and specific impulse. However, it is impractical to determine the HOF of novel energetic materials because of their unstable intermediates and unknown combustion mechanism. The calculated total energies (E_0), zero-point energies (*ZPE*), and thermal corrections (H_T) at the M06-2X/def2-TZVPP level for the reference and target compounds used in isodesmic reactions are listed in Table S1. The gas phase *HOFs* (HOF_{Gas}) have been predicted by designing appropriate isodesmic reactions. In an isodesmic reaction, the number of each kind of formal bond is conserved according to bond separation reaction (*BSR*) rules. The target molecule is broken down into a set of heavy atom molecules containing same component bonds. BSR rules cannot be applied to the molecules with delocalized bonds and cage skeletons because of large calculated errors of *HOFs*. In view of the above, present study

involves the design of isodesmic reactions in which FOX-7 core kept invariable to decrease the calculation errors of *HOF*. The usage of the HOF_{Gas} in the calculation of detonation properties slightly overestimates the values of detonation velocity and detonation pressure, and hence, the solid phase *HOF* (HOF_{Solid}) has been calculated which can efficiently reduce the errors. The HOF_{Solid} is calculated as the difference between HOF_{Gas} and heat of sublimation (HOF_{Sub}) as,

$$HOF_{Solid} = HOF_{Gas} - HOF_{Sub} \quad (1)$$

The heat of sublimation (HOF_{Sub}), which is required to convert the HOF_{Gas} to the HOF_{Solid}, was calculated from Equation (2),[2]

$$HOF_{Sub} = 0.000267\,A^2 + 1.650087\left(v\sigma_{tot}^2\right)^{0.5} - 2.966078 \quad (2)$$

where, A represents the surface area of the 0.001 electrons/bohr^3 isosurface of electronic density, v denotes the degree of balance between the positive and negative surface potentials, and σ_{tot}^2 is the electrostatic potential variance. These molecular surface properties were obtained using the Multiwfn program[3] and listed in Table S2. The heats of sublimation for FOX-7 and 2T-FOX are 119.4 and 125.21 kJ/mol, respectively.

Table S1. Calculated total energies (E_0), zero-point energies (*ZPE*), thermal correction (H_T), and HOF_{Gas} for the reference and target compounds.

Reference Compd.	E_0	*ZPE*	H_T	HOF_{GAS}

	(a.u.)	(a.u.)	(a.u.)	(kJ/mol)
FOX-7	-598.233189	0.0935	0.1037	9.95
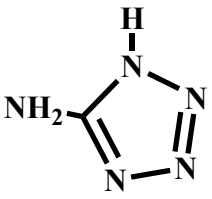	-313.547217	0.0647	0.0698	323.80[a]
NH_3	-56.513652	0.034518	0.0038	-45.9[a]
2T-FOX	-1112.261432	0.1506	0.0168	749.47

[a]Obtained from http://webbook.nist.gov

Table S2. Calculated molecular surface properties of FOX-7 and 2T FOX.

Compd.	Surface area ($Å^2$)	Volume ($Å^3$)	σ^2_{tot} (kcal/mol)	σ^2_+ (kcal/mol)	σ^2_- (kcal/mol)	Balance Parameter (ν)
FOX-7	150.97	143.68	429.37	334.97	94.39	0.1715
2T-FOX	250.63	262.74	417.78	375.47	42.31	0.0910

Surface area and volume are computed on the 0.001 au molecular surfaces. σ^2_{tot} indicate the variability of the electrostatic potential, σ^2_+ denote the variance of the positive surface potentials, σ^2_- denote the variance of the negative surface potentials, and ν is the degree of balance between the positive and the negative potentials on a molecular surface and is unitless.

The density has been referred to as "the primary physical parameter in detonation performance" of explosives[4-10]. For example, the important performance attribute of detonation velocity is proportional to density, while the detonation pressure is proportional to the square of the initial density[11,12]. An increase in density is also desirable in terms of the amount of material that can be packed into volume-limited warhead or propulsion

configurations. The densities (ρ) for designed compounds were calculated using the Polymorph module in Materials Studio with Dreiding forcefield. Oxygen balance (*OB*) is one of the parameter of quantifying how well an explosive provides its own oxidant[13]. Most of the energy released comes from oxidation (reaction with oxygen), the amount of oxygen available is a critical factor. If excess oxygen molecules are remaining after the oxidation reaction, the oxidizer is said to have a 'positive' *OB*. If the oxygen molecules are completely consumed and excess fuel molecules remain, the oxidizer is said to have a 'negative' *OB*. If neutral *OB* (*OB* = 0%), means that there is exactly enough oxygen for the complete oxidation. It is reported that the heat of detonation (*Q*) reaches a maximum for an *OB* of zero, since this corresponds to the stoichiometric oxidation of carbon to carbon dioxide and hydrogen to water. The *OB* can therefore be used to optimize the composition of the explosive to give an *OB* as close to zero as possible. In addition, knowledge of *OB* in explosives can be applied is in the processing of mixtures of explosives. *OB* (%) for an explosive containing the general formula $C_aH_bN_cO_d$ with molecular mass *M* can be calculated as,

$$OB(\%) = \frac{(d - 2a - 0.5b)}{M} X\ 1600 \qquad (4)$$

A prime concern in the area of energetic materials (explosives and propellants) is sensitivity. Sensitivity refers to the vulnerability of a material to unintended detonation due to an accidental stimulus (impact, shock, electrical sparks, etc.) [14-21]. Sensitivity depends upon a number of different factors: molecular and crystal properties, the physical state of the compound, environmental conditions, the nature of the stimulus, etc. Partly for these reasons, reproducibility of measured values is notoriously difficult. Experimentally, great care is required to employ very specific and uniform procedures and conditions in preparing and testing the materials; and most of the times these procedures provide crude and qualitative

estimates. In view of the computational work, a large number of correlations have been established between different types of sensitivity and a remarkable array of individual molecular or crystal properties. These properties include the strengths or lengths of certain bonds, electronic energy levels, molecular electrostatic potentials, heats of fusion or sublimation, band gaps, *NMR* chemical shifts, the efficiencies of lattice-to molecular vibrational energy transfer, atomic charges, electronegativities, substituent constants, etc. In the present work, we used the bond dissociation energies (*BDEs*) value to correlate the thermal stability of energetic molecules. In energetic materials, generally, C–NO_2, N–NO_2 and O–NO_2 are the weakest bond which easily ruptures on applying external stimuli. In previous reports, evidence indicates that a key initiation step is the rupture of a specific type of bond, a "trigger linkage". Hence, we have calculated the bond dissociation energy (*BDE*) of longest N–NO_2 bond using following equation (5) at M06-2X/def2-TZVPP level,

$$BDE = [E_{R1} + E_{R2}] - E_{R1-R2} \quad (5)$$

where E_{R1-R2}, $E_{R1,}$ and E_{R2} are the total energies with zero-point energy correction of the precursor and the corresponding radicals produced by bond dissociation (see Table S3). Politzer et al.[22] established the correlation between free space in the crystal lattice (ΔV) of energetic material and sensitivity. The computed overall surface area, positive and negative electrostatic potentials of FOX-7 and 2T-FOX are listed in Table S4. The free space per molecule was calculated by subtracting the effective volume per molecule (V_{eff}) and the intrinsic gas phase molecular volume (V_{int}) as given in Eq. (6),

$$\Delta V = V_{eff} - V_{int} \quad (6)$$

For the safe handling, transport, and storage of high-energy materials (HEMs), newly developed compounds must demonstrate sufficient stability and insensitivity to meet the

necessary standards. Politzer et al.[23] proposed an equation for Impact sensitivity (h_{50}), based on statistically defined molecular electrostatic potential parameters given in Eq. (7). h_{50} refers to the height (in cm) from which a standard weight dropped on an explosive material has a 50% chance of initiation or detonation. higher (h_{50}) value is preferred as lower h_{50} values indicate greater sensitivity, meaning the material is more likely to initiate when subjected to impact.

$$h_{50} = \left(-0.0064\sigma_{+}^{2} \right) + 241.42\nu - 3.43 \quad (7)$$

σ_{+}^{2} represents the positive variance, and ν signifies the balance of charges between the positive and negative surface potentials.

Table S3. Calculated total energies (E_0) of R–NO_2, R, and NO_2 at the M06-2X/def2-TZVPP level, used in the prediction of bond dissociation energies.

Compound	***E₀* (a.u.)**		
	R-NO_2	**R**	**NO_2**
FOX-7	-598.233189	-393.052090	-205.064437
2T-FOX	-1112.261432	-907.100596	-205.064437

Table S4. Calculated overall surface area, positive and negative electrostatic potentials of FOX-7 and 2T-FOX.

Compd.	**Overall surface area (Å²)**	**Positive surface area (Å²)**	**Negative surface area (Å²)**	**Positive Potential (%)**	**Negative Potential (%)**
FOX-7	150.97	77.04	73.92	51	49
2T-FOX	250.63	128.42	122.21	51	49

QTAIM Analysis

The topological analysis of electron densities was performed by using atoms in molecules (AIM) theory.[24-26] The wave functions extracted from the M06-2X/def2-TZVPP level calculation was used to compute the electron density (ρ) and the corresponding Laplacian ($\nabla^2\rho$) values at the bond critical points (*BCPs*). Table S5 summarize the computed *QTAIM* topological parameters at the (3, -1) bond critical point for the FOX-7 and 2T-FOX. The characteristics of the bond critical point (*BCP*) were obtained in terms of the electron density (ρ) and its Laplacian (($\nabla^2\rho$) at the critical point, the total electron-energy density (H_{BCP}), the electron potential energy density (V_{BCP}), and the Lagrangian kinetic energy (G_{BCP}). The relations between these parameters are shown in equations (8) and (9):

$$\frac{1}{4}\nabla^2\rho = 2G_{BCP} + V_{BCP} \quad (8)$$

$$H_{BCP} = G_{BCP} + V_{BCP} \quad (9)$$

The hydrogen-bond energy (E_H) was obtained by using Equation (10), proposed by Espinosa et al.[27]

$$E_H = V_{BCP}/2 \quad (10)$$

Table S5. Computed *QTAIM* topological parameters at the (3, -1) bond critical point for the FOX-7 and 2T-FOX using M06-2X/def2-TZVPP level of theory.

Compd	CP	Interaction	Bond Length (Å)	ρ_{BCP} (au)	G_{BCP} (au)	V_{BCP} (au)	$\nabla^2\rho_{BCP}$ (au)	H_{BCP} (au)	$-G/V$ (au)
FOX-7	33	N1-H2…O3	1.83	0.037	0.035	-0.037	0.133	-0.002	0.947
	15	N7-H8…O9	1.83	0.037	0.035	-0.037	0.133	-0.002	0.947

2T-FOX	48	N1-H2…O3	2.01	0.023	0.022	-0.020	0.097	0.002	1.109
	49	N4-H5…O6	2.01	0.023	0.022	-0.020	0.097	0.002	1.111

Table S6. Reported physicochemical, energetic and safety properties of various FOX-7 derivatives (shown in Figure 1).

Compound	***HOF*[a] *(kJ/mol)***	***ρ*[b] *(g/cm³)***	***T*$_d$[c] *(⁰C)***	***D*[d] *(km/s)***	***P*[e] *(GPa)***	***IS*[f] *(J)***	***FS*[g] *(N)***	**Ref.**
i	35.4	1.88	164	8.94	35.4	20	240	[28]
ii	-175.0	1.90	75	8.9	37.7	17	-	[29,30]
iii	55.8	1.90	135	8.8	35.8	20	240	[29,31]
iv	-260.9	1.75	-	8.6	32.1	19.6	16	[32]
v	-	-	-	-	-	-	-	[32,33,34]
vi	-	-	-	-	-	-	-	[35]
vii	-	-	-	-	-	-	-	[35]
viii	-	-	-	-	-	-	-	[35]
ix	-74.2	1.79	209.2	8.28	28.9	>40	>360	[35]
x	61.8	1.65	-	7.9	23.2	>40	>360	[35,36]
xi	71.6	1.78	124.5	8.80	33.8	6	-	[37,38]
xii	-	-	-	-	-	-	-	[37]

[a]Heat of formation (kJ/mol), [b]Density (g/cm^3), [c]Decomposition temperature (°C), [d]Detonation velocity (km/s), [e]Detonation pressure (GPa), [f] Impact sensitivity (J), [g]Friction sensitivity (N).

Designed isodesmic reaction

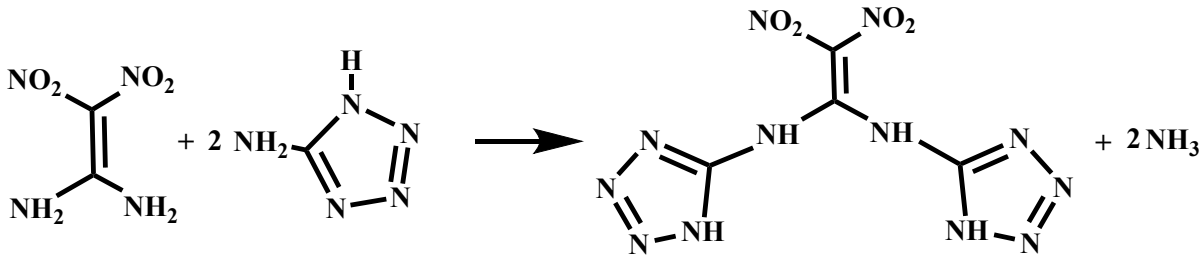

Figure S1. Designed isodesmic reaction for the 2T-FOX.

Optimized structures with selective bond lengths and angles

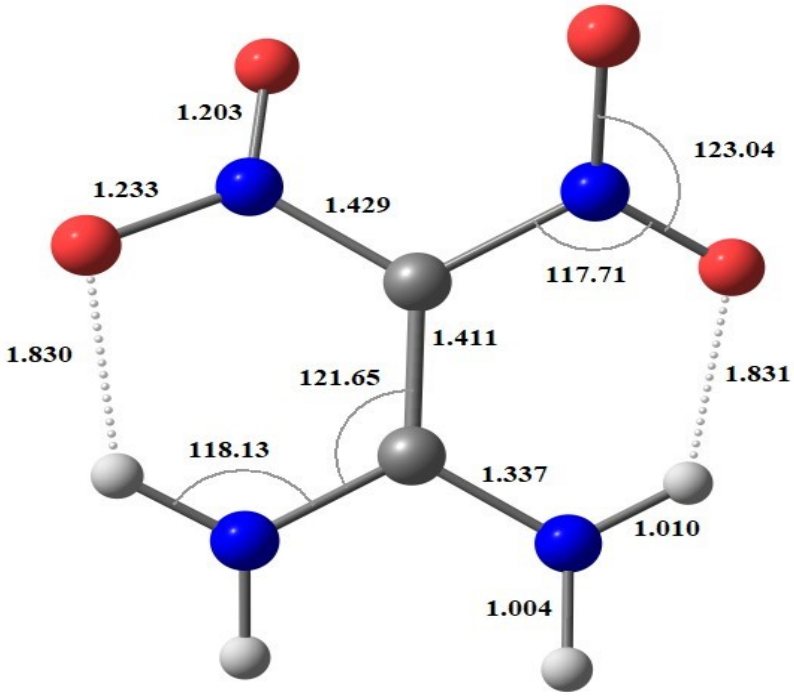

Figure S2. Selective bond lengths (Å) and angles (˚) in FOX-7

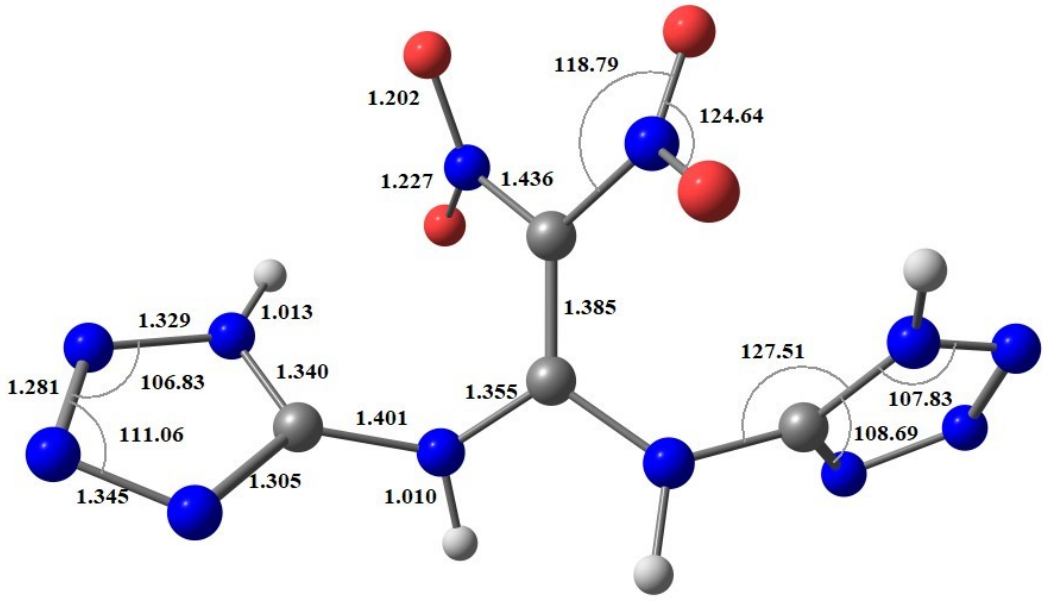

Figure S3. Selective bond lengths (Å) and angles (˚) in 2T-FOX.

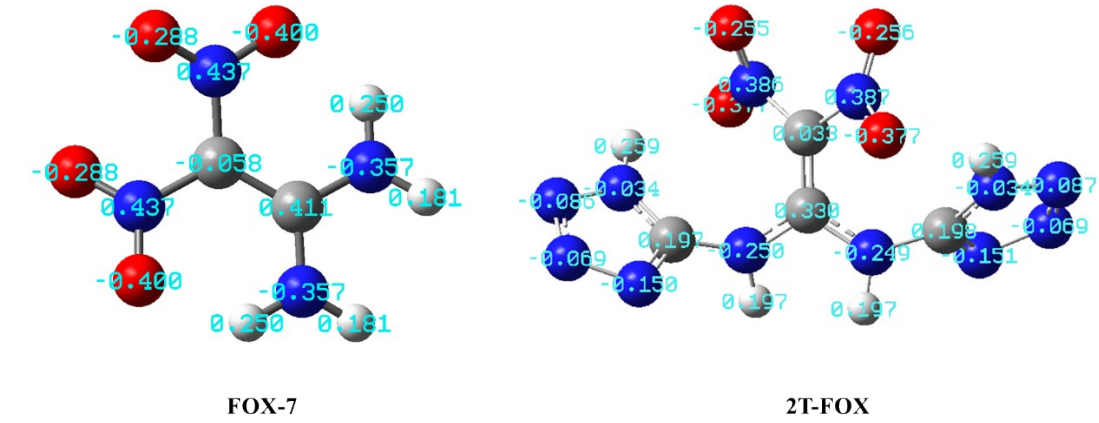

Figure S4. Mulliken charge distribution of FOX-7 and 2T-FOX.

Optimized Cartesian coordinates

Table S7. Optimized coordinates of **FOX-7** at M06-2X/def2-TZVPP level of theory.

6	1.362323000	0.000238000	-0.000139000
6	-0.048825000	0.000034000	-0.000225000
7	-0.803568000	1.209890000	0.097484000

8	-0.255969000	2.257230000	-0.253957000
8	-1.915903000	1.172502000	0.554134000
7	-0.803083000	-1.210163000	-0.097587000
8	-1.915544000	-1.173291000	-0.553970000
8	-0.254976000	-2.257163000	0.254015000
7	2.064019000	-1.130799000	0.126662000
7	2.063790000	1.131458000	-0.126604000
1	3.048998000	-1.127725000	-0.065692000
1	1.556416000	-1.994020000	0.255969000
1	3.048682000	1.128610000	0.066207000
1	1.555951000	1.994573000	-0.255763000

Table S8. Optimized coordinates of **2T-FOX** at M06-2X/def2-TZVPP level of theory.

6	0.001197000	-0.596971000	0.000836000
6	-0.000763000	0.787626000	-0.000493000
7	1.094114000	-1.332010000	0.319205000
7	-1.090563000	-1.334296000	-0.316538000
6	2.422077000	-1.041104000	-0.021482000
7	3.076958000	-1.659960000	-0.965062000
7	3.255520000	-0.191495000	0.593322000
7	4.326488000	-1.164461000	-0.922659000
7	4.440447000	-0.281815000	-0.001793000
6	-2.418727000	-1.043525000	0.023663000
7	-3.254747000	-0.201884000	-0.598738000
7	-3.071295000	-1.654187000	0.974137000

7	-4.438680000	-0.288511000	-0.001411000
7	-4.321833000	-1.161664000	0.928253000
1	0.929060000	-2.292005000	0.586316000
1	-0.924268000	-2.293800000	-0.584598000
1	3.078430000	0.438314000	1.366929000
1	-3.079180000	0.422337000	-1.377209000
7	0.879900000	1.549612000	0.839469000
8	1.246400000	2.630491000	0.463974000
8	1.226782000	1.022570000	1.891477000
7	-0.885204000	1.544188000	-0.842073000
8	-1.260570000	2.621909000	-0.466344000
8	-1.225674000	1.015577000	-1.895278000

References

1. M. J. Frisch, G. W. Trucks, H. B. Schlegel, G. E. Scuseria, M. A. Robb, J. R. Cheeseman, G. Scalmani, V. Barone,G. A. Petersson, H. Nakatsuji, X. Li, M. Caricato, A. Marenich, J. Bloino, B. G. Janesko, R. Gomperts, B. Mennucci, H. P. Hratchian, J. V. Ortiz, A. F. Izmaylov, J. L. Sonnenberg, D. Williams-Young, F. Ding, F. Lipparini, F. Egidi, J. Goings, B. Peng, A. Petrone, T. Henderson, D. Ranasinghe, V. G. Zakrzewski, J. Gao, N. Rega, G. Zheng, W. Liang, M. Hada, M. Ehara, K. Toyota, R. Fukuda, J. Hasegawa, M. Ishida, T. Nakajima, Y. Honda, O. Kitao, H. Nakai, T. Vreven, K. Throssell, J. A. Montgomery Jr, J. E. Peralta, F. Ogliaro, M. Bearpark, J. J. Heyd, E. Brothers, K. N. Kudin, V. N. Staroverov, T. Keith, R. Kobayashi, J. Normand, K. Raghavachari, A. Rendell, J. C. Burant, S. S. Iyengar, J. Tomasi, M. Cossi, J. M. Millam, M. Klene, C. Adamo, R. Cammi, J. W. Ochterski, R. L. Martin, K. Morokuma, O. Farkas, J. B. Foresman and D. J. Fox, *Gaussian 09, Revision E.01*, Gaussian, Inc., Wallingford, CT, 2013.

2. E. F. C. Byrd and B. M. Rice, *J. Phys. Chem. A*, 2005, **110**, 1005–1013.
3. T. Lu and F. Chen, *J. Comput. Chem.*, 2011, **33**, 580–592.
4. H. D. B. Jenkins, D. Tudela and L. Glasser, *Inorg. Chem.*, 2002, **41**, 2364–2367.
5. S. Beaucamp, N. Marchet, D. Mathieu *et al.*, *Acta Crystallogr., Sect. B: Struct. Sci., Cryst. Eng. Mater.*, 2003, **59**, 498–504.
6. C. M. Tarver, *J. Chem. Eng. Data*, 1979, **24**, 136–145.
7. C. Ye and J. M. Shreeve, *J. Chem. Eng. Data*, 2008, **53**, 520–524.
8. C. Ye and J. M. Shreeve, *J. Phys. Chem. A*, 2007, **111**, 1456–1461.
9. B. M. Rice and D. C. Sorescu, *J. Phys. Chem. B*, 2004, **108**, 17730–17739.
10. P. Politzer and J. S. Murray, *Cent. Eur. J. Energ. Mater.*, 2017, **14**, 3–25.
11. M. J. Kamlet and S. J. Jacobs, *J. Chem. Phys.*, 1968, **48**, 23–35.
12. P. Politzer, J. Martinez, J. S. Murray *et al.*, *Mol. Phys.*, 2009, **107**, 2095–2101.
13. H. Muthurajan and A. H. Ghee, *Cent. Eur. J. Energ. Mater.*, 2008, **5**, 19–35.
14. C. B. Storm, J. R. Stine and J. F. Kramer, in *Chemistry and Physics of Energetic Materials*, ed. S. Bulusu, Springer, Dordrecht, 1990, pp. 605–639.
15. R. Meyer, J. Köhler and A. Homburg, *Explosives*, Wiley-VCH, Weinheim, 6th edn, 2007.
16. M. Sućeska, *Test Methods for Explosives*, Springer, New York, 1995.
17. B. M. Rice and J. J. Hare, *J. Phys. Chem. A*, 2002, **106**, 1770–1783.
18. P. Politzer and J. S. Murray, in *Energetic Materials, Part 2: Detonation, Combustion*, ed. P. Politzer and J. S. Murray, Elsevier, Amsterdam, 2003, ch. 6.
19. R. M. Doherty and D. S. Watt, *Propellants Explos. Pyrotech.*, 2008, **33**, 4–13.
20. M. Pospíšil, P. Vávra, M. C. Concha *et al.*, *J. Mol. Model.*, 2011, **17**, 2569–2574.
21. J. S. Murray, M. C. Concha and P. Politzer, *Mol. Phys.*, 2009, **107**, 89–97.
22. P. Politzer and J. S. Murray, *J. Mol. Model.*, 2014, **20**, 2223.

23. Pospíšil M., Vávra P., Concha M. C., Murray J. S., Politzer P., *J. Mol. Model*., 2009, **16**, 895–901.

24. C. R. Wick and T. Clark, *J. Mol. Model.*, 2018, **24**, 142.

25. S. Shahbazian, *Chem. Eur. J.*, 2018, **24**, 5401–5405.

26. X. Zhang and X. Gong, *ChemPhysChem*, 2014, **15**, 2281–2287.

27. E. Espinosa, E. Molins and C. Lecomte, *Chem. Phys. Lett.*, 1998, **285**, 170–173.

28. C. Yan, H. Yang, X. Qi, Y. Jin, K. Wang, T. Liu, J. Tian, F. Nie, G. Cheng and Q. Zhang, *Chem. Commun*., 2018, **54**, 9333–9336.

29. S. Banik, A. Kumar Yadav, P. Kumar, V. D. Ghule and S. Dharavath, *Chem. Eng. J*., 2022, ***431***, 133378.

30. A. E. Frumkin, N. V. Yudin, K. Yu. Suponitsky and A. B. Sheremetev, *Mendeleev Commun*., 2018, **28**, 135–137.

31. C. Yan, G. Cheng, K. Wang, T. Liu, Y. Jin, H. Yang and Q. Zhang, *New J. Chem*., 2019, **43**, 10429–10433.

32. T. Zhou, Y. Li, K. Xu, J. Song and F. Zhao, *New J. Chem*., 2017, **41**, 168–176.

33. J. N. She, K. Z. Xu, H. Zhang, J. Huang, F. Q. Zhao, and J. R. Song, *Acta Chim. Sinica*, 2009, **67**, 2645.

34. K. Z. Xu, H. Zhang, P. Liu, J. Huang, Y. H. Ren, B. Z. Wang and F. Q. Zhao, *Propellants Explos. Pyrotech.*, 2012, **37**, 653.

35. H. Gao and J. M. Shreeve, *RSC Adv*., 2016, **6**, 56271–56277.

36. Y. Xu, C. Shen, Q. Lin, P. Wang, C. Jiang and M. Lu, *J. Mater. Chem. A*, 2016, 4, 17791–17800.

37. A. K. Chinnam, R. J. Staples and J. M. Shreeve, *Org. Lett*., 2021, **23**, 76–80.

38. S. Lal, R. J. Staples and J. M. Shreeve**,** *Chem. Eng. J.***,** 2023**, 452,** 139600.